

## New strategies to improve the luminescence efficiency of Eu ions embedded in Si-based matrices

S. Boninelli, G. Bellocchi, G. Franzò, M. Miritello, and F. Iacona

Citation: [Journal of Applied Physics](#) **113**, 143503 (2013); doi: 10.1063/1.4799407

View online: <http://dx.doi.org/10.1063/1.4799407>

View Table of Contents: <http://scitation.aip.org/content/aip/journal/jap/113/14?ver=pdfcov>

Published by the [AIP Publishing](#)

---

### Articles you may be interested in

[Influences of doping and annealing conditions on the photoluminescence from In<sub>2</sub>O<sub>3</sub> nanocrystals and Eu<sup>3+</sup> ions co-doped sol-gel SiO<sub>2</sub> films](#)

J. Appl. Phys. **109**, 083512 (2011); 10.1063/1.3569889

[Energy transfer and enhanced luminescence in metal oxide nanoparticle and rare earth codoped silica](#)

Appl. Phys. Lett. **92**, 201109 (2008); 10.1063/1.2936842

[Switchable two-color electroluminescence based on a Si metal-oxide-semiconductor structure doped with Eu](#)

Appl. Phys. Lett. **90**, 181121 (2007); 10.1063/1.2735285

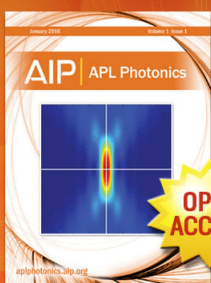
[Site of Er ions in silica layers codoped with Si nanoclusters and Er](#)

Appl. Phys. Lett. **88**, 121915 (2006); 10.1063/1.2190267

[Precipitation-induced photostimulated luminescence in CsBr : Eu<sup>2+</sup>](#)

J. Appl. Phys. **93**, 5109 (2003); 10.1063/1.1563303

---



Launching in 2016!  
The future of applied photonics research is here

**AIP** | APL  
Photonics

# New strategies to improve the luminescence efficiency of Eu ions embedded in Si-based matrices

S. Boninelli,<sup>1,a)</sup> G. Bellocchi,<sup>1,2</sup> G. Franzò,<sup>1</sup> M. Miritello,<sup>1</sup> and F. Iacona<sup>1</sup>

<sup>1</sup>MATIS IMM CNR, via Santa Sofia 64, 95121 Catania, Italy

<sup>2</sup>Dipartimento di Fisica e Astronomia, Università di Catania, via Santa Sofia 64, 95121 Catania, Italy

(Received 23 January 2013; accepted 20 March 2013; published online 8 April 2013)

The comparison of the performances of SiO<sub>2</sub> and SiOC layers as host matrices for optically active Eu ions is presented. A SiO<sub>2</sub> matrix allows to observe light emission from both Eu<sup>2+</sup> and Eu<sup>3+</sup> ions, owing to a proper tuning of the thermal annealing process used for the optical activation of the rare earth. However, the photoluminescence efficiency of both ions remains relatively low and quite far from the requirements for technological applications, mainly due to the extensive formation of Eu-containing precipitates. A detailed study by transmission electron microscopy allowed us to analyze and elucidate the clustering process and to find suitable strategies for minimizing it. We found that the substitution of SiO<sub>2</sub> matrix with a SiOC film allows to obtain a very bright light emission centered at about 440 nm from Eu<sup>2+</sup> ions. In fact, SiOC is able to efficiently promote the Eu<sup>3+</sup> → Eu<sup>2+</sup> reduction; furthermore, Eu ions are characterized by an enhanced mobility and solubility in this matrix, and as a consequence, Eu precipitation is strongly reduced. Since SiOC is a material fully compatible with standard Si technology, Eu-doped SiOC layers can be considered a highly interesting candidate for photonic applications. © 2013 American Institute of Physics. [<http://dx.doi.org/10.1063/1.4799407>]

## I. INTRODUCTION

The intense and stable emission in the visible region exhibited by Eu ions is currently successfully applied in phosphors used in lighting technology.<sup>1–6</sup> Indeed, one of the most common approaches used to generate white light in light emitting diodes (LEDs) exploits the combination of an UV- or blue-emitting LED with a suitable phosphor layer where both Eu<sup>2+</sup> and Eu<sup>3+</sup> ions act as emitting centers at different wavelengths. However, the low Eu solid solubility represents an important limit for the practical applications of this rare earth, and a very wide research field deals with the search for innovative host matrices able to accommodate higher and higher Eu concentrations.<sup>7,8</sup> The existence of two different stable Eu oxidation states widens the range of Eu applications, but it may involve also relevant drawbacks; indeed, this peculiarity can be really considered an advantage only if it is possible to selectively obtain the desired species or, for specific applications,<sup>9</sup> determine the co-existence of the two states. The Eu<sup>3+</sup> emission consists of some narrow lines (the most intense is in the red spectral region at about 615 nm) originating from dipole-forbidden transitions; therefore, it has a remarkably lower intensity with respect to the wide emission band of Eu<sup>2+</sup>, whose maximum can be found in the wavelength range 400–600 nm, and it is due to dipole-allowed transitions. Eu users are, therefore, somewhat forced to choose between the sharp emission peaks of Eu<sup>3+</sup> and the high emission efficiency of Eu<sup>2+</sup>, although the exploiting of efficient energy transfer processes between a properly chosen matrix and the rare earth ions has been successfully proposed as a way to increase the efficiency of the Eu<sup>3+</sup> emission process.<sup>10,11</sup>

Also potential Eu applications in Si photonics, including the fabrication of light sources or optical amplifiers, have to cope with the presence of two oxidation states; this property differentiates Eu from other rare earth ions widely used in photonics, such as Er or Yb, which are stable only in the trivalent oxidation state. Furthermore, an additional primary requirement to be faced is the true compatibility of the Eu-containing material with CMOS processing; the simplest road that has been followed is represented by the insertion of Eu ions as dopant in a Si oxide matrix,<sup>12–16</sup> analogously to the well established case of Er.<sup>17</sup> In particular, Skorupa and co-workers extensively studied the properties of electroluminescent MOS devices based on Eu-doped SiO<sub>2</sub> layers exploiting the emission from both Eu<sup>2+</sup> and Eu<sup>3+</sup> ions,<sup>12–15</sup> but even the success of this approach is strongly prevented by the low Eu solid solubility, which leads to massive phenomena of Eu clustering and precipitation.<sup>13–16</sup>

In agreement with the above considerations and in spite of the promising emission properties, the interest around Eu seems to be mainly confined to the field of phosphors, where solubility issues can be largely solved owing to the peculiar properties of novel host matrices. However, either the composition of these matrices, spanning from simple oxides, such as Y<sub>2</sub>O<sub>3</sub> or Gd<sub>2</sub>O<sub>3</sub>,<sup>18</sup> to rather complex compounds, such as YCa<sub>3</sub>(AlO)<sub>3</sub>(BO<sub>3</sub>)<sub>4</sub>,<sup>19</sup> or the techniques used for their synthesis (mainly sol-gel methods) are, in general, very far from being considered compatible with current Si technology. The main challenge for Eu application in photonics is, therefore, represented by the availability of a host matrix, whose synthesis and processing are compatible with Si technology, which is simultaneously capable to efficiently host high concentrations of optically active Eu ions, and that allows the control of the Eu oxidation state.

<sup>a)</sup>Electronic mail: simona.boninelli@ct.infn.it

Aim of this work is the comparison of the performances of a pure SiO<sub>2</sub> and of a SiOC matrix (which, also given its low C content, around 5 at. %, can be considered fully compatible with Si technology) as hosts for optically active Eu ions, in view of applications in photonics of Eu-containing materials. It will be shown that in the case of a SiO<sub>2</sub> matrix, although both Eu<sup>2+</sup> and Eu<sup>3+</sup> emissions can be obtained, the photoluminescence (PL) efficiency remains quite far from requirements for practical applications, due to the extensive formation of Eu-containing precipitates. On the other hand, it will be shown that a SiOC matrix, owing to its chemical (i.e., the capability to efficiently promote the Eu<sup>3+</sup> → Eu<sup>2+</sup> reduction) and structural (Eu ions benefit from enhanced mobility and solubility and this strongly reduces Eu precipitation) properties, is able to ensure an intense and stable light emission centered at about 440 nm from Eu<sup>2+</sup> ions, which could be of great interest for photonic applications.

## II. EXPERIMENTAL

Eu-doped SiO<sub>2</sub> thin films were grown on (100) Si substrates heated at 400 °C by using an ultrahigh vacuum magnetron sputtering system. The base pressure was about  $1 \times 10^{-9}$  mbar. The deposition has been obtained by rf co-sputtering of 4 in. diameter, water-cooled SiO<sub>2</sub> and Eu<sub>2</sub>O<sub>3</sub> targets (99.9% purity or higher). The deposition was carried out with a sputter up configuration in a  $5 \times 10^{-3}$  mbar Ar atmosphere. Sputter rates have been set in order to obtain two Eu concentrations ( $1.5$  and  $5.0 \times 10^{20} \text{ cm}^{-3}$ ). Eu-doped SiOC thin films were grown by rf co-sputtering of SiO<sub>2</sub>, SiC, and Eu<sub>2</sub>O<sub>3</sub> targets (99.9% purity or higher). Sputter rates have been set in order to obtain a C concentration of about 5 at. % and an Eu concentration of  $1.5 \times 10^{20} \text{ cm}^{-3}$ . Both SiO<sub>2</sub>- and SiOC-based films are about 200 nm thick. After deposition, samples were thermally treated for 1 h in ultra-pure O<sub>2</sub> or N<sub>2</sub> ambient by using a horizontal furnace operating at temperatures ranging from 750 to 1000 °C.

Transmission electron microscopy (TEM) analysis in bright field (BF) mode, performed by a 200 kV Jeol 2010 microscope, was used to investigate the film structure, while a 200 kV Jeol 2010F microscope, equipped with a Gatan Image Filter, was used to investigate the chemical composition by energy filtered TEM (EFTEM) analyses.

The atomic composition of the films was studied by Rutherford backscattering spectrometry (RBS), using a 2 MeV He<sup>+</sup> beam in random configuration, with a detector placed at 165° with respect to the incident beam.

PL measurements were performed by pumping with the 325 nm line of a He-Cd laser. The pump power was about 3 mW, and the laser beam was chopped through an acousto-optic modulator at a frequency of 55 Hz. The PL signal was analyzed by a single grating monochromator and detected with a Hamamatsu visible photomultiplier. Spectra were recorded with a lock-in amplifier using the acousto-optic modulator frequency as a reference. All the spectra have been measured at room temperature and corrected for the spectral system response.

## III. RESULTS AND DISCUSSION

### A. Eu-doped SiO<sub>2</sub> matrix

The problem of the low Eu solubility in a SiO<sub>2</sub> matrix is made worse by the thermal process required to maximize the emission properties of the system. Thermal annealing is unavoidable when Eu ions are introduced by ion implantation,<sup>14</sup> since this process removes implantation damage (which may generate non-radiative de-excitation channels) and makes optically active the Eu ions by optimizing their chemical environment.<sup>13</sup> However, a thermal annealing can be very useful also when, as in the present case, a non-damaging technique such as co-sputtering, is used to dope the material.

Cluster formation in Eu-doped SiO<sub>2</sub> and its dependence on the thermal annealing conditions are illustrated in Fig. 1. The BF cross sectional TEM (XTEM) image reported in Fig. 1(a) shows that no precipitation occurs in a SiO<sub>2</sub> film doped with  $5.0 \times 10^{20} \text{ Eu/cm}^3$  and annealed at 750 °C in N<sub>2</sub>. The same scenario is found for processes performed at temperatures lower than 750 °C and in as-deposited samples. On

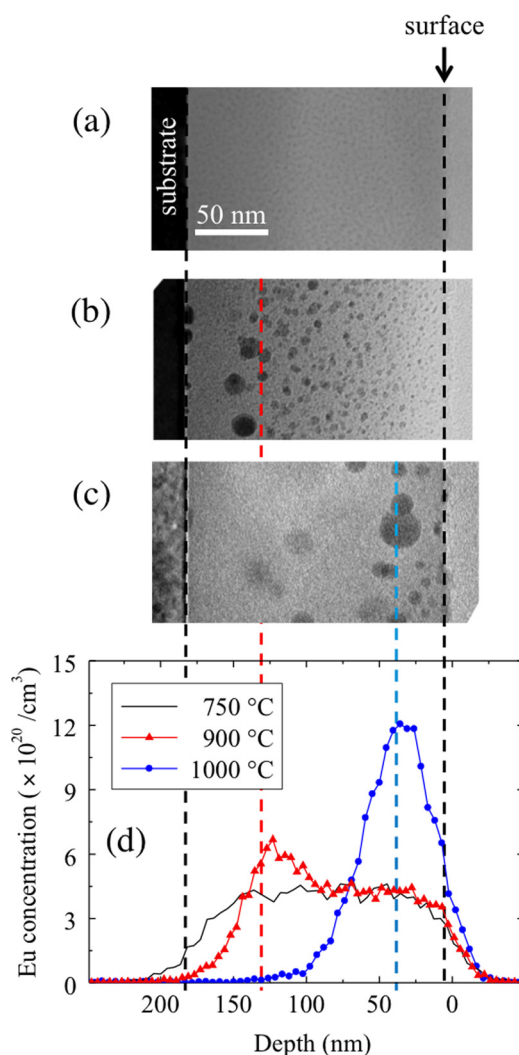


FIG. 1. BF XTEM images relative to Eu-doped SiO<sub>2</sub> films annealed in N<sub>2</sub> ambient at (a) 750 °C, (b) 900 °C, and (c) 1000 °C. Eu concentration is  $5.0 \times 10^{20} \text{ cm}^{-3}$  in all cases. (d) Eu concentration profiles, measured by RBS, relative to the samples shown in panels (a)-(c).



the other hand, precipitate formation is clearly visible in the BF XTEM images referring to samples annealed at 900 and 1000 °C in N<sub>2</sub> (see Figs. 1(b) and 1(c), respectively). At 900 °C, clusters are almost homogeneously distributed throughout the film, but their size markedly decreases on going from the interface with the substrate (where diameters as large as about 15 nm are found) towards the surface (where the mean diameter is few nm). At 1000 °C, most of the precipitates are found close to the surface and a marked increase of their maximum diameter (about 30 nm) occurs.

Eu precipitation is tightly related to Eu diffusion toward the surface, as demonstrated by the analysis of the Eu concentration profiles, measured by RBS, reported in Fig. 1(d). The Eu profile of the sample annealed at 750 °C (black line) is almost constant throughout the SiO<sub>2</sub> layer, indicating the absence of relevant diffusion phenomena at this temperature. At 900 °C (red line and triangles), an Eu peak located at a depth of about 125 nm (corresponding to the region where the larger precipitates are detected in the TEM image) emerges over the Eu background concentration. At 1000 °C (blue line and circles), the Eu peak is more intense and moves towards the surface, at a depth of about 30 nm, corresponding again to the region where the larger precipitates are detected by TEM, while in the deeper regions, the residual Eu concentration is very low. In all cases, the total detected Eu concentration does not change with respect to the as-deposited sample, indicating the absence of Eu outdiffusion phenomena.

In order to gain more information about the nature and composition of the precipitates, further TEM investigations have been performed. Fig. 2(a) shows a BF XTEM image, taken at a higher magnification with respect to the image in Fig. 1(b), of an Eu-doped SiO<sub>2</sub> sample containing  $5.0 \times 10^{20}$  Eu/cm<sup>3</sup> and treated at 900 °C in N<sub>2</sub> atmosphere. Since no information about the cluster composition can be extracted from a conventional TEM image, we have employed also the EFTEM technique. In Fig. 2(b), the EFTEM map of elemental Eu, obtained by energy filtering at 133 eV (corresponding to the N<sub>IV</sub> edge of Eu) and by using the 3-windows method,<sup>20</sup> is shown; the image displays exactly the same region of Fig. 2(a) and unambiguously demonstrates that all clusters contain Eu.

The diffraction pattern reported in the inset of Fig. 2(a) indicates that the Eu-containing precipitates are amorphous

or strongly damaged. Since high resolution (HR) TEM conducted on several tens of clusters was not able to detect the typical fringes of the crystalline planes, we can conclude that all clusters are amorphous. The only crystalline clusters are detected at the interface with the Si substrate, as shown by the HR TEM image reported in Fig. 2(c), referring to the cluster circled in red in Fig. 2(b). The analysis of the corresponding fast Fourier transform (FFT), shown in Fig. 2(d), reveals that these precipitates are epitaxial with respect to the Si substrate. Moreover, the simulation of the FFT, superimposed in Fig. 2(d) as red circles, allows to recognize that these clusters have the crystalline structure of pure Eu<sub>2</sub>O<sub>3</sub>. The experimental evidences on the nature of the interfacial clusters, coupled with the well known tendency of rare earth ions, including Eu and Er, to precipitate as an oxidized phase when they are embedded in SiO<sub>2</sub>,<sup>21,22</sup> allow us to reasonably conclude that also the amorphous precipitates consist of Eu oxides (and/or silicates).

Eu precipitation in SiO<sub>2</sub> is not a surprising phenomenon, since it is well known that it has a low solid solubility in this matrix.<sup>14,16,21</sup> On the other hand, the peculiar temperature dependence of the precipitation phenomenon (both size and position of the clusters remarkably change) and the tendency of the clusters to move towards the surface when the annealing temperature is increased are certainly less expected. In the as-deposited sample, the Eu ions are homogeneously distributed throughout the film; during the thermal process, they acquire mobility but, in the absence of any concentration gradient, no relevant diffusion process is expected. However, we have to take into account that Eu ions tend to be fully coordinated with O atoms. Furthermore, a non-negligible oxygen contamination is unavoidably present in the conventional furnaces used for thermal processing in Si-based technology, even if ultra-pure N<sub>2</sub> is used. This implies that oxygen diffuses inside the samples but, given its low concentration, it is reasonable to assume that it is mainly present in the surface region of the film. Therefore, the higher oxygen concentration close to the surface and the tendency of Eu ions to be surrounded by O atoms to stabilize their chemical environment, both concur to force Eu migration towards the surface, as shown in Fig. 1. Under these conditions, Eu solubility in SiO<sub>2</sub> is largely overcome and clustering occurs.

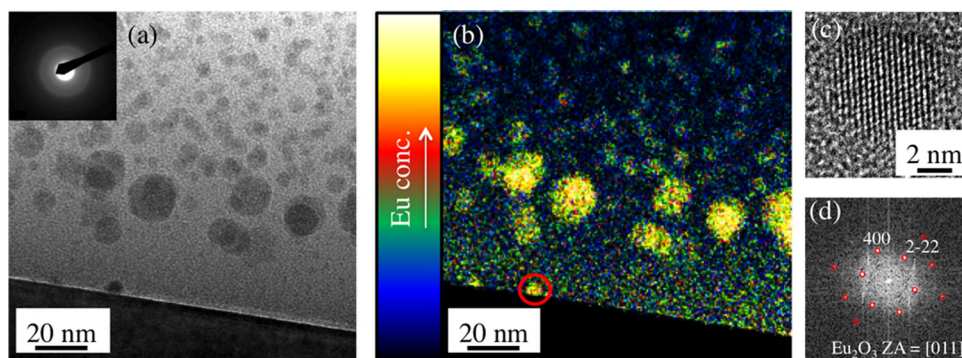


FIG. 2. (a) BF XTEM image relative to an Eu-doped SiO<sub>2</sub> film (Eu concentration is  $5.0 \times 10^{20}$  cm<sup>-3</sup>) annealed in N<sub>2</sub> ambient at 900 °C. In the inset, the electron diffraction pattern of the same sample is shown. (b) EFTEM cross section image showing the same region of the same sample shown in panel (a), obtained by energy filtering at 133 eV (corresponding to the N<sub>IV</sub> edge of Eu). (c) HR TEM image of the precipitate circled in red in panel (b). (d) Fast Fourier transform of the cluster shown in panel (c); the red circles are the simulation of the FFT.

To confirm the role of oxygen as a driving force for Eu migration towards the surface, annealing processes in pure O<sub>2</sub> ambient have been performed. In particular, an Eu-doped SiO<sub>2</sub> sample containing  $5.0 \times 10^{20}$  Eu/cm<sup>3</sup> has been annealed in O<sub>2</sub> ambient at 900 °C. The BF XTEM image of this sample, shown in Fig. 3(a), if compared with that of Fig. 1(b), clearly shows that clustering, although still present, is deeply influenced by the change of the environment of the annealing process. In the same figure, the Eu concentration profile, obtained from RBS data, is superimposed to the XTEM image, and indicates a homogeneous Eu depth distribution and the absence of Eu diffusion towards the surface. The precipitation phenomenon can be better described by using cross section EFTEM images; the Eu map shown in Fig. 3(b), obtained by energy filtering at 133 eV, evidences a huge number of very small Eu-containing precipitates (mean diameter is about 5 nm) uniformly dispersed throughout the film. The above behaviour depends on the capability of oxygen to diffuse inside the whole film; under these conditions, Eu ions have no reasons to move, and the precipitation phenomenon shown in Fig. 3 depends only on the overcoming of the Eu solubility in SiO<sub>2</sub>. Since this scenario is strongly different with respect to that characterizing samples annealed in N<sub>2</sub> ambient, we can conclude that oxygen plays a key role during the annealing of Eu-doped SiO<sub>2</sub>.

In order to correlate the structural and the optical properties of Eu-doped SiO<sub>2</sub> films, we have performed PL measurements. Fig. 4 shows the PL spectra of as-deposited and annealed films, obtained at room temperature by exciting the samples with the 325 nm line of a He-Cd laser. The PL spectrum of the as-deposited sample consists of a broad band having its maximum at about 435 nm, corresponding to the emission of Eu<sup>2+</sup> ions,<sup>23</sup> and of some narrow lines corresponding to the emission of Eu<sup>3+</sup> ions.<sup>3</sup> The most intense Eu<sup>3+</sup> line is found at 616 nm with a FWHM of about 15 nm and corresponds to the <sup>5</sup>D<sub>0</sub> → <sup>7</sup>F<sub>2</sub> transition of Eu<sup>3+</sup> ions in solid matrices; the less intense peaks at about 578, 590, 656, and 704 nm correspond to <sup>5</sup>D<sub>0</sub> → <sup>7</sup>F<sub>J</sub> transitions, with J = 1, 3, 4, and 5, respectively. After annealing the samples in N<sub>2</sub> ambient, we notice an increased intensity of the peak associated to Eu<sup>2+</sup>, coupled with a shift to 450 nm (at 750 °C) and

to 475 nm (at 900 °C); a further increase of the PL intensity and a small redshift are found at 1000 °C (spectrum not shown). The Eu<sup>3+</sup> emission remains clearly visible as a peak at 750 °C and as a shoulder of the Eu<sup>2+</sup> peak at 900 °C. The increased PL intensity in annealed samples accounts for a reduced density in the host matrix of defects which can constitute preferential channels for non-radiative de-excitation and for a better Eu coordination, while the peak redshift is related to the formation of regions characterized by different local Eu concentrations.<sup>24,25</sup> We recall indeed that while the emission of Eu<sup>3+</sup> is due to 4f-intrashell transition and does not depend on the chemical environment of the ion, the emission of Eu<sup>2+</sup> is due to a 4f-5d transition sensible to local variation of the Eu chemical environment.<sup>26</sup> The co-existence of Eu<sup>2+</sup> and Eu<sup>3+</sup> ions in Eu-doped SiO<sub>2</sub> is not surprising; indeed, the different nature of the Eu<sup>2+</sup> and Eu<sup>3+</sup> emissions (the first is due to an allowed transition, the second to a forbidden one) leads to an overestimation of the Eu<sup>2+</sup> content, if this estimate is based on the relative intensities of their characteristic PL features. This means that even a small oxygen deficiency can determine the presence of an Eu<sup>2+</sup> signal having an intensity comparable to that one of Eu<sup>3+</sup>.

On the other hand, from the analysis of Fig. 4, it appears evident that in samples annealed in O<sub>2</sub> the Eu<sup>2+</sup> peak fully disappears, due to the complete oxidation of Eu<sup>2+</sup> in Eu<sup>3+</sup>. We notice also a marked increase by about a factor of 10 of the PL intensity for the Eu<sup>3+</sup>-related peaks in the sample annealed at 750 °C in O<sub>2</sub> with respect to the as-deposited one. A decrease of the PL intensity accounting for a factor of 2 is found when the annealing temperature is increased to 900 °C, contrarily to what happens for N<sub>2</sub> processes, where a monotonic increase as a function of the temperature is observed. This effect depends on the higher effectiveness of oxygen with respect to the temperature in eliminating the matrix defects that may act as non-radiative de-excitation channels, by maximizing the yield of the photon emission process already at 750 °C. As a consequence, a further increase of the

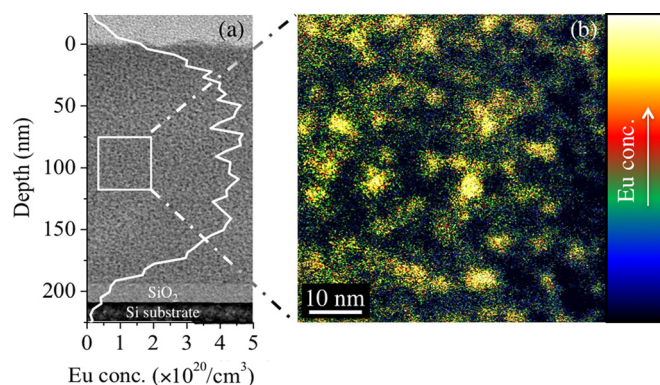


FIG. 3. (a) BF XTEM image relative to an Eu-doped SiO<sub>2</sub> film (Eu concentration is  $5.0 \times 10^{20}$  cm<sup>-3</sup>) annealed in O<sub>2</sub> ambient at 900 °C. The Eu concentration profile, measured by RBS, is superimposed to the image. (b) EFTEM Eu map showing a detail of the sample shown in panel (a), obtained by energy filtering at 133 eV (corresponding to the N<sub>IV</sub> edge of Eu).

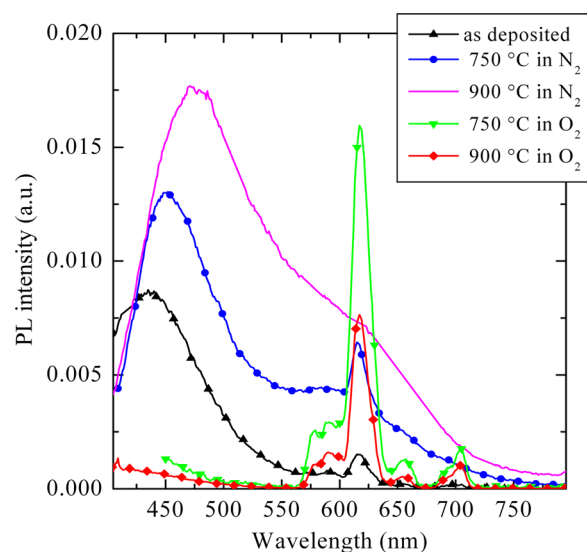


FIG. 4. Room temperature PL spectra of Eu-doped SiO<sub>2</sub> films (Eu concentration is  $5.0 \times 10^{20}$  cm<sup>-3</sup>) as-deposited and annealed at 750 and 900 °C, both in N<sub>2</sub> and O<sub>2</sub> ambient.



annealing temperature produces only a decrease of the emission intensity due to the occurrence of clustering phenomena, in agreement with the TEM data shown in Fig. 3.

By summarizing, the structural data concerning Eu-doped SiO<sub>2</sub> highlight the occurrence of Eu precipitation in samples annealed both in O<sub>2</sub> and in N<sub>2</sub> environments. Although it is clear that this phenomenon strongly limits the fraction of optically active Eu ions, it is also evident that, due to the defects present in the matrix, a thermal process is required to optimize the optical properties of the system. This need is demonstrated by the stronger PL signals exhibited by annealed samples, even if the thermal process simultaneously induces Eu precipitation. Since it is well known that Eu compounds can be very efficient light emitters,<sup>27,28</sup> a question arises about the possibility that the PL signals from Eu-doped SiO<sub>2</sub> come (at least in part) from the Eu-containing clusters formed during the annealing processes. At this purpose, our experimental evidences are in some way contradictory; indeed, on one hand, we observe a PL signal also from precipitate-free samples (films as-deposited or annealed at temperatures of 750 °C or lower), and on the other hand, the increase of the PL intensity by increasing the annealing temperature of N<sub>2</sub> processes, shown in Fig. 4, could suggest that precipitates have an active role in the light emission process. Our opinion is that precipitates are optically inactive; indeed, the previously reported strong light emission from Eu compounds, such as oxides or silicates, has been linked to the presence of crystalline structures.<sup>16,27</sup> In the present case, since most of precipitates are amorphous (and very reasonably they have not a well defined stoichiometry), their optical inactivity appears strongly probable. Further arguments about the optical properties of Eu precipitates will be given in the following of the manuscript.

Eu precipitation and the prevalence of the Eu<sup>3+</sup> oxidation state both concur in making the optical properties of Eu-doped SiO<sub>2</sub> films quite far from the requirements for application of this material for the fabrication of Si-based light sources. A straightforward approach to solve at least the problem of Eu precipitation could be the reduction of its concentration. The result of this attempt is illustrated in the BF XTEM images reported in Figs. 5(a) and 5(c), referring to a SiO<sub>2</sub> film containing  $1.5 \times 10^{20}$  Eu/cm<sup>3</sup> (i.e., an Eu concentration which is more than 3 times lower than that present in the samples discussed above), annealed in N<sub>2</sub> at 900 and 1000 °C, respectively. The TEM images show that Eu precipitation is still present; precipitate position is very similar to that found in samples containing a higher Eu concentration, but a marked decrease of their size and density is obtained. Although these improved structural properties also produce a moderate increase of the PL intensity (accounting for less than a factor of 2 at 900 °C), it seems clear that further improvements are needed.

## B. Eu-doped SiOC matrix

We have developed a new approach to make SiO<sub>2</sub> a better host for Eu ions. It has been widely reported in literature that the Eu solubility can be remarkably increased by properly modifying (from both chemical and structural points of

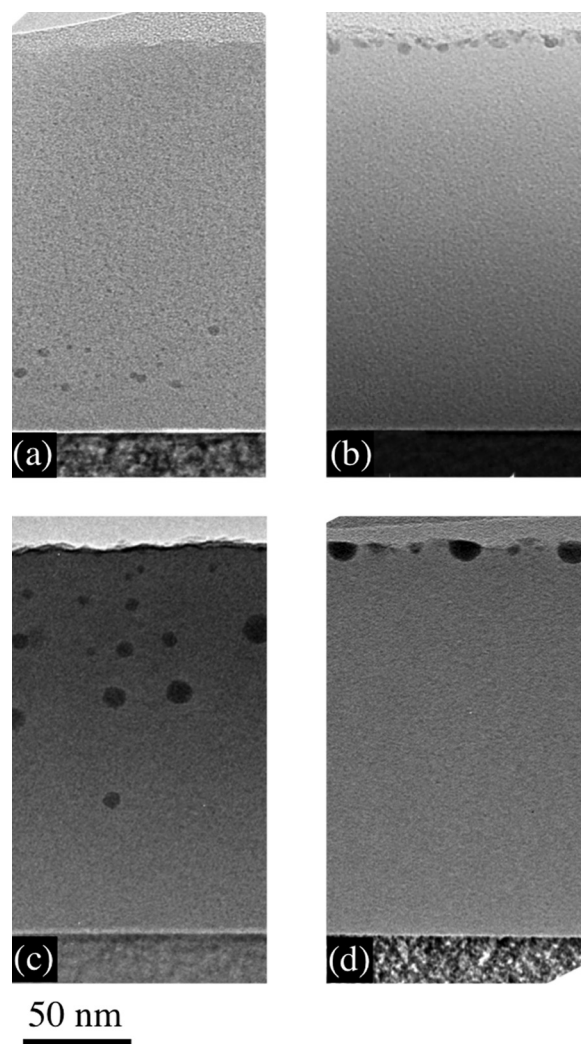


FIG. 5. BF XTEM images relative to (a) Eu-doped SiO<sub>2</sub> annealed in N<sub>2</sub> ambient at 900 °C; (b) Eu-doped SiOC annealed in N<sub>2</sub> ambient at 900 °C; (c) Eu-doped SiO<sub>2</sub> annealed in N<sub>2</sub> ambient at 1000 °C; (d) Eu-doped SiOC annealed in N<sub>2</sub> ambient at 1000 °C. Eu concentration is  $1.5 \times 10^{20}$  cm<sup>-3</sup> in all of the samples.

view) the host matrix.<sup>21,29,30</sup> Since the high luminescence efficiency of Eu<sup>2+</sup> ions can be more appealing for our purposes, we have modified our matrix in order to simultaneously increase the Eu solubility and efficiently induce the Eu<sup>3+</sup> → Eu<sup>2+</sup> reduction, by moving from a pure SiO<sub>2</sub> to a SiOC matrix, having a C content of about 5 at. %. There are several good reasons for choosing a SiOC matrix: (i) it has been already shown to be a good host for rare earth ions, including Er,<sup>31</sup> Eu,<sup>32</sup> and Tb;<sup>33</sup> (ii) C is a reducing agent and can be used to promote the Eu<sup>3+</sup> → Eu<sup>2+</sup> reduction;<sup>23</sup> (iii) SiC is a semiconductor, so we expect, similarly to the well known Si addition to SiO<sub>2</sub>,<sup>34</sup> an improved electrical conduction in SiOC with respect to SiO<sub>2</sub>, which could make the material also suitable for the fabrication of electroluminescent devices; (iv) SiC is a wide bandgap semiconductor, so a possible effect of indirect Eu excitation through energy transfer from SiC nanoclusters (nc's) could be sought for, similarly to what happens in Er-doped Si nc.<sup>35</sup>

The SiOC matrix seems to be very effective in increasing Eu solubility, as demonstrated in Fig. 5, comparing the

BF XTEM images relative to Eu-doped SiO<sub>2</sub> and SiOC films annealed at 900 (Figs. 5(a) and 5(b)) and 1000 °C (Figs. 5(c) and 5(d)) in N<sub>2</sub> ambient. The Eu concentration is  $1.5 \times 10^{20} \text{ cm}^{-3}$  for all the samples. From the analysis of the figure, it is evident that SiC addition dramatically changes the structural properties of the Eu-doped SiO<sub>2</sub> films. Indeed, for both the explored annealing temperatures, cluster formation occurs now only at the sample surface. Precipitates have been studied by electron diffraction and EFTEM analyses, and analogously to what found for the pure SiO<sub>2</sub> matrix, they contain Eu and are amorphous. No precipitation occurs in as-deposited samples.

RBS measurements allow the quantitative analysis of the Eu precipitation process in the SiOC matrix. Fig. 6 shows the comparison between the Eu concentration profiles, obtained from RBS spectra, relative to an as-deposited Eu-doped SiOC film (black line) and those corresponding to thermally annealed samples (900 °C, red line and triangles; 1000 °C, blue line and circles, both in N<sub>2</sub> environment). The data in Fig. 6 show a uniform Eu depth distribution in the as-deposited film and confirm the occurrence of Eu surface segregation in annealed samples evidenced also by the TEM images in Fig. 5. The surface Eu concentration peaks account for about 10% (at 900 °C) and 65% (at 1000 °C) of the total Eu concentration (values estimated by subtracting a background equal to the Eu concentration in the deeper film regions). Even in this case, no Eu out-diffusion has been evidenced. Since Eu precipitates are confined in a very thin surface region, they can be also visualized by using plan view TEM analysis without the occurrence of any overlap between clusters. In Fig. 7, a plan view BF TEM image of an Eu-doped SiOC film annealed at 1000 °C (the corresponding XTEM image is shown in Fig. 5(d)) is reported. The image shows a high density of well resolved, almost circular precipitates. The total volume of the precipitates can be easily evaluated; from this information, however, the fraction of clustered Eu ions cannot be unambiguously derived, since the precipitate composition is unknown. Alternatively, by using the tabulated densities for the most common Eu

compounds containing O and/or Si, we can estimate that an Eu fraction ranging from 40% (by hypothesizing the presence of the Eu compound characterized by the lowest Eu density, i.e., the silicate EuSiO<sub>3</sub> (Ref. 36)) to 85% (if the Eu compound characterized by the highest Eu density, i.e., the oxide EuO,<sup>37</sup> is present) is contained in the precipitates. Both values are in good agreement with the RBS estimate obtained from the data in Fig. 6. Although a fraction of precipitated Eu roughly ranging from 40% to 85% (at 1000 °C) could appear very high, we have to remember that the dissolved fraction corresponds, at worst, to an Eu concentration of about  $2.2 \times 10^{19} \text{ cm}^{-3}$ , which remains a very high solubility value with respect to those reported in literature for rare earth ions dissolved in the most common SiO<sub>2</sub>-based matrices.<sup>38</sup>

The peculiar behaviour of Eu in SiOC is due to the combined effect of oxygen (which, analogously to the case of the pure SiO<sub>2</sub> matrix, activates Eu diffusion towards surface) and of an enhanced Eu mobility in the SiOC matrix. This enhanced Eu diffusion must be necessarily taken into account, since the precipitates detected at the surface have a total Eu content which largely exceeds that present in the surface region in the absence of diffusion processes. Under these conditions, a very high Eu concentration is gathered in the surface layers, leading to the extensive cluster formation shown by the TEM images in Figs. 5 and 7.

On the basis of the above considerations, it is important to obtain a reduction of the oxygen influence during the thermal annealing of Eu-doped SiOC films in order to fully exploit the enhanced Eu solubility in this matrix. The strategy we followed is the deposition of a SiO<sub>2</sub> capping layer (200 nm thick) on Eu-doped films before the annealing step, in order to avoid as much as possible additional Eu-O interactions. The effect of the capping layer on Eu behaviour is shown by the BF XTEM images relative to SiO<sub>2</sub>-capped SiOC (a) and SiO<sub>2</sub> (b) samples annealed at 900 °C in N<sub>2</sub> reported in Fig. 8. Eu concentration is  $1.5 \times 10^{20} \text{ cm}^{-3}$  in both cases. It is very remarkable the fact that the capping layer is able to completely suppress Eu precipitation in a SiOC matrix, as clearly shown by Fig. 8(a). In the same

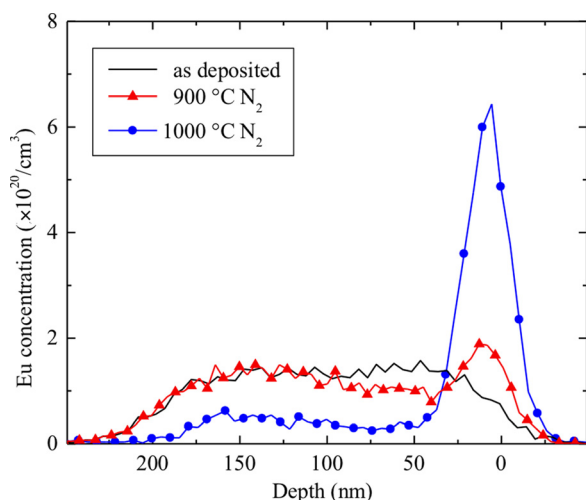


FIG. 6. Eu concentration profiles, measured by RBS, relative to Eu-doped SiOC films as-deposited and annealed in N<sub>2</sub> ambient at 900 and 1000 °C. Eu concentration is  $1.5 \times 10^{20} \text{ cm}^{-3}$  in all of the samples.

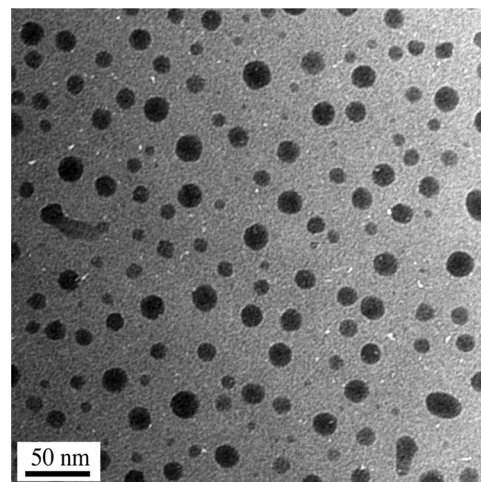


FIG. 7. Plan view BF TEM image of an Eu-doped SiOC film annealed in N<sub>2</sub> ambient at 1000 °C. Eu concentration is  $1.5 \times 10^{20} \text{ cm}^{-3}$ .

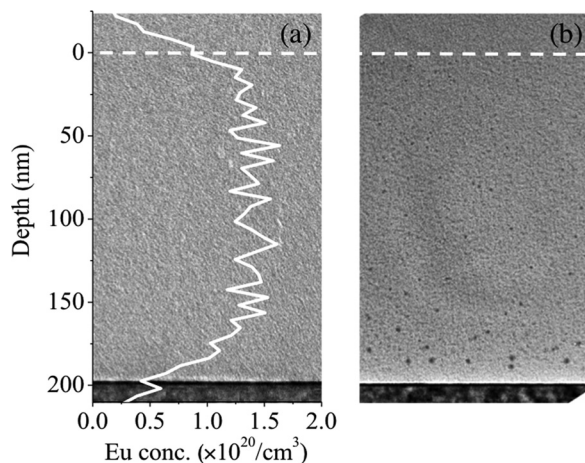


FIG. 8. (a) BF XTEM image of Eu-doped SiOC annealed in  $N_2$  ambient at  $900^\circ\text{C}$  after the deposition of a  $\text{SiO}_2$  capping layer. The Eu concentration profile, extracted from the RBS spectrum, is superimposed to the TEM image. (b) BF XTEM image of an Eu-doped  $\text{SiO}_2$  annealed in  $N_2$  ambient at  $900^\circ\text{C}$  after the deposition of a  $\text{SiO}_2$  capping layer. The dashed line indicated the position of the interface between the Eu-doped films and the  $\text{SiO}_2$  capping layer. Eu concentration is  $1.5 \times 10^{20} \text{ cm}^{-3}$  in all of the samples.

figure, the Eu concentration profile (obtained from RBS spectra), showing that Eu is uniformly dispersed inside the film, is overlapped to the TEM image. On the other hand, the  $\text{SiO}_2$  capping layer is less effective in avoiding Eu precipitation in a pure  $\text{SiO}_2$  matrix; indeed, the XTEM image reported in Fig. 8(b) shows the presence of residual Eu-containing precipitates close to the interface with the Si substrate. This experiment demonstrates that in a situation in which Eu is not subjected to any diffusion process, the SiOC matrix is able to fully prevent Eu precipitation.

Data shown in Figs. 5–8 clearly illustrate the complex structural evolution induced by the addition of SiC to a  $\text{SiO}_2$  matrix, and, above all, how the capability of the matrix to dissolve high Eu concentration is deeply (and positively) affected. Furthermore, the SiOC matrix is also able to efficiently promote the  $\text{Eu}^{3+} \rightarrow \text{Eu}^{2+}$  reduction. The room temperature PL spectra of several different Eu-doped SiOC samples containing  $1.5 \times 10^{20} \text{ Eu/cm}^3$  are reported in Fig. 9. All the spectra are characterized by two common features: (i) they have very similar shapes, corresponding to  $\text{Eu}^{2+}$  emission, and only quite small intensity variations and wavelength shifts among the various peaks can be noted. No peaks or shoulders assignable to the presence of  $\text{Eu}^{3+}$  can be detected. (ii) All PL peaks are much more intense (by more than two orders of magnitude) than those relative to the Eu-doped  $\text{SiO}_2$  samples.

More in detail, the PL spectrum of an Eu-doped SiOC sample annealed at  $900^\circ\text{C}$  in  $N_2$  (red dashed line) can be compared with that of a  $\text{SiO}_2$  sample containing the same Eu content and annealed under the same conditions (shown in Fig. 9 multiplied by a factor of 100—black line and up triangles). A very strong enhancement of the room temperature PL emission of about a factor of 250 has been obtained; furthermore, the peak is sharper and its maximum, detected at about 435 nm, is blue-shifted by about 60 nm. By increasing the annealing temperature of Eu-doped SiOC samples up to  $1000^\circ\text{C}$ , no relevant variation of the PL emission is found;

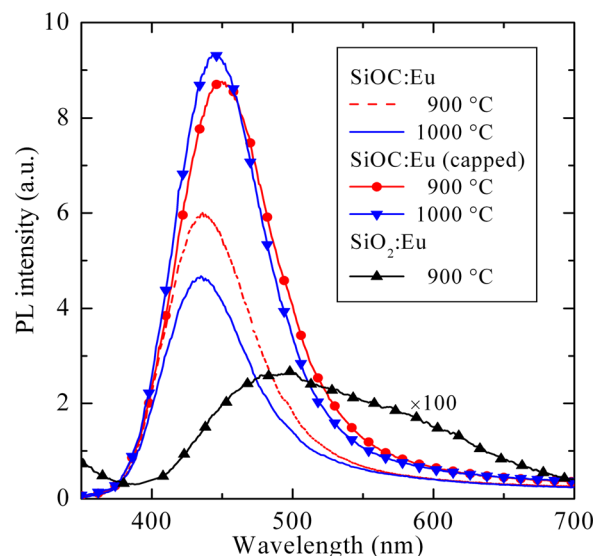


FIG. 9. Room temperature PL spectra of Eu-doped SiOC and  $\text{SiO}_2$  films annealed at 900 and  $1000^\circ\text{C}$  in  $N_2$  ambient. The PL spectrum of Eu-doped  $\text{SiO}_2$  is multiplied by a factor of 100. In the case of SiOC, spectra of both  $\text{SiO}_2$ -capped and uncapped samples are shown. Eu concentration is  $1.5 \times 10^{20} \text{ cm}^{-3}$  in all of the samples.

indeed, the PL spectrum (blue line in Fig. 9) appears almost unchanged both in shape and in position and the small decrease of the PL intensity (about 20%) is in agreement with the presence of a higher precipitate density evidenced by the TEM and RBS data in Figs. 5–7. Fig. 9 also reports the PL spectra of Eu-doped SiOC samples annealed at  $900^\circ\text{C}$  (red circles and line) and  $1000^\circ\text{C}$  (blue down triangles and line) after the  $\text{SiO}_2$  cap deposition. In agreement with the capability of the capping layer to fully prevent Eu precipitation, demonstrated by the XTEM image in Fig. 8(a), a further enhancement of the PL intensity, accounting for about a factor of 2, has been obtained for both temperatures.

Similarly to what discussed above for the case of the  $\text{SiO}_2$  matrix, also in the case of the SiOC matrix, the observation of strong PL signals from samples characterized by the presence of Eu-containing precipitates rises the question on their possible optical activity. Although the arguments we have previously presented to exclude this effect maintain their validity also for the SiOC matrix, we have been able to collect also a clear experimental evidence of the lack of relevant light emission from Eu-containing clusters. Indeed, the fact that, differently from the  $\text{SiO}_2$  matrix, all the precipitates detected in SiOC are located in a thin (about 10 nm) surface region, allowed us to remove them by using a low energy, rastered Ar ion source. The observation that, also after cluster removal, the PL properties of the samples are unchanged constitutes a strong evidence of the fact that only the Eu ions which are dissolved in the matrix are optically active. Moreover, this experiment supports the above reported considerations about the need of a well defined stoichiometry and/or crystalline structure to make optically active the Eu-containing precipitates.

#### IV. CONCLUSIONS

In this paper, limits and perspectives of pure  $\text{SiO}_2$  and SiOC matrices as a host for optically active Eu ions have



been presented and discussed. In the case of SiO<sub>2</sub>, both Eu<sup>2+</sup> and Eu<sup>3+</sup> emissions have been obtained, but the occurrence of an extensive Eu precipitation in thermally annealed films seems to be unavoidable. The formation of Eu-containing clusters has been studied in a great detail, and the role played by the temperature and by the chemical environment during the thermal treatment of this material elucidated. Although some strategies for minimizing clustering phenomena and improving the efficiency of the light emission process have been proposed, the material remains quite far from requirements for practical applications.

On the other hand, a SiOC matrix is able to efficiently promote the Eu<sup>3+</sup> → Eu<sup>2+</sup> reduction, so enriching the system with the Eu species exhibiting the brightest luminescence. Furthermore, TEM and RBS data have demonstrated that Eu ions in SiOC are characterized by an enhanced mobility and solubility; this peculiarity leads to a strongly reduced Eu precipitation and, as a consequence, to a very intense and stable light emission at about 440 nm, from Eu<sup>2+</sup> ions. Since SiOC can be fully considered a material compatible with Si technology and an appreciable electrical conduction is expected in this matrix, we believe that Eu-doped SiOC films may open new and interesting perspectives for photonic applications of Eu-containing materials.

## ACKNOWLEDGMENTS

The authors wish to thank F. Priolo (MATIS IMM CNR) for fruitful discussions, A. Scandurra and G. Indelli (Consorzio Catania Ricerche) and G. Mannino (IMM CNR) for collaboration to some of the experiments reported in the article.

- <sup>1</sup>A. Kitai, *Luminescent Materials and Applications* (John Wiley & Sons Ltd., 2008).
- <sup>2</sup>K.-W. Huang, W.-T. Chen, C.-I. Chu, S.-F. Hu, H.-S. Sheu, B.-M. Cheng, J.-M. Chen, and R.-S. Liu, *Chem. Mater.* **24**, 2220 (2012).
- <sup>3</sup>Y. Tian, B. Chen, R. Hua, J. Sun, L. Cheng, H. Zhong, X. Li, J. Zhang, Y. Zheng, T. Yu, L. Huang, and H. Yu, *J. Appl. Phys.* **109**, 053511 (2011).
- <sup>4</sup>X. Ye, W. Zhuang, Y. Hu, T. He, X. Huang, C. Liao, S. Zhong, Z. Xu, H. Nie, and G. Deng, *J. Appl. Phys.* **105**, 064302 (2009).
- <sup>5</sup>Y. Q. Li, A. C. A. Delsing, G. de With, and H. T. Hintzen, *Chem. Mater.* **17**, 3242 (2005).
- <sup>6</sup>N. Hirosaki, R.-J. Xie, K. Kimoto, T. Sekiguchi, Y. Yamamoto, T. Suehiro, and M. Mitomo, *Appl. Phys. Lett.* **86**, 211905 (2005).
- <sup>7</sup>T. Higuchi, Y. Hotta, Y. Hikita, S. Maruyama, Y. Hayamizu, H. Akiyama, H. Wadati, D. G. Hawthorn, T. Z. Regier, R. I. R. Blyth, G. A. Sawatzky, and H. Y. Hwang, *Appl. Phys. Lett.* **98**, 071902 (2011).

- <sup>8</sup>C.-J. Jia, L.-D. Sun, F. Luo, X.-C. Jiang, L.-H. Wei, and C.-H. Yan, *Appl. Phys. Lett.* **84**, 5305 (2004).
- <sup>9</sup>Z.-Y. Mao, D.-J. Wang, Q.-F. Lu, W.-H. Yub, and Z.-H. Yuan, *Chem. Commun.* **2009**(3), 346.
- <sup>10</sup>S. P. Singh and B. Karmakar, *RSC Adv.* **1**, 751 (2011).
- <sup>11</sup>Z. Xia, J. Zhuang, and L. Liao, *Inorg. Chem.* **51**, 7202 (2012).
- <sup>12</sup>S. Prucnal, J. M. Sun, W. Skorupa, and M. Helm, *Appl. Phys. Lett.* **90**, 181121 (2007).
- <sup>13</sup>L. Rebohle, J. Lehmann, S. Prucnal, A. Kanjilal, A. Nazarov, I. Tyagulskaa, W. Skorupa, and M. Helm, *Appl. Phys. Lett.* **93**, 071908 (2008).
- <sup>14</sup>L. Rebohle, J. Lehmann, S. Prucnal, A. Nazarov, I. Tyagulskaa, S. Tyagulskaa, A. Kanjilal, M. Voelskow, D. Grambole, W. Skorupa, and M. Helm, *J. Appl. Phys.* **106**, 123103 (2009).
- <sup>15</sup>A. N. Nazarov, S. I. Tyagulskaa, I. P. Tyagulskaa, V. S. Lysenko, L. Rebohle, J. Lehmann, S. Prucnal, M. Voelskow, and W. Skorupa, *J. Appl. Phys.* **107**, 123112 (2010).
- <sup>16</sup>D. Li, X. Zhang, L. Jin, and D. Yang, *Opt. Express* **18**, 27191 (2010).
- <sup>17</sup>A. Polman, *J. Appl. Phys.* **82**, 1 (1997).
- <sup>18</sup>B. Antic, J. Rogan, A. Kremenovic, A. S. Nikolic, M. Vucinic-Vasic, D. K. Bozanic, G. F. Goya, and P. Colomban, *Nanotechnology* **21**, 245702 (2010).
- <sup>19</sup>L. Wang and Y. Wang, *Mater. Sci. Eng., B* **139**, 232 (2007).
- <sup>20</sup>O. L. Krivanek, M. K. Kundmann, and X. Bourrat, *Mater. Res. Soc. Symp. Proc.* **332**, 341 (1994).
- <sup>21</sup>N. D. Afify and G. Mountjoy, *Phys. Rev. B* **79**, 024202 (2009).
- <sup>22</sup>M. W. Sckerl, S. Guldberg-Kjaer, M. Ryscholt Poulsen, P. Shi, and J. Chevallier, *Phys. Rev. B* **59**, 13494 (1999).
- <sup>23</sup>Y. Qiao, D. Chen, J. Ren, B. Wu, J. Qiu, and T. Akai, *J. Appl. Phys.* **103**, 023108 (2008).
- <sup>24</sup>X. Song, H. He, R. Fu, D. Wang, X. Zhao, and Z. Pan, *J. Phys. D: Appl. Phys.* **42**, 065409 (2009).
- <sup>25</sup>X. Song, R. Fu, S. Agathopoulos, H. He, X. Zhao, and S. Zhang, *J. Appl. Phys.* **106**, 033103 (2009).
- <sup>26</sup>G. Blasse and B. C. Grabmaier, *Luminescent Materials* (Springer-Verlag, Berlin, 1994).
- <sup>27</sup>G. Bellocchi, G. Franzò, F. Iacona, S. Boninelli, M. Miritello, T. Cesca, and F. Priolo, *Opt. Express* **20**, 5501 (2012).
- <sup>28</sup>Y. C. Shin, S. J. Leem, C. M. Kim, S. J. Kim, Y. M. Sung, C. K. Hahn, J. H. Baek, and T. G. Kim, *J. Electroceram.* **23**, 326 (2009).
- <sup>29</sup>Y. Kishimoto, X. Zhang, T. Hayakawa, and M. Nogami, *J. Lumin.* **129**, 1055 (2009).
- <sup>30</sup>Q. Zhang, X. Liu, Y. Qiao, B. Qian, G. Dong, J. Ruan, Q. Zhou, J. Qiu, and D. Chen, *Opt. Mater.* **32**, 427 (2010).
- <sup>31</sup>S. Gallis, M. Huang, H. Efsthadiadis, E. Eisenbraun, A. E. Kaloyeros, E. E. Nyein, and U. Hommerich, *Appl. Phys. Lett.* **87**, 091901 (2005).
- <sup>32</sup>Y. J. Zhang, A. Quaranta, and G. D. Soraru, *Opt. Mater.* **24**, 601 (2004).
- <sup>33</sup>S.-Y. Seo and J. H. Shin, *Appl. Phys. Lett.* **84**, 4379 (2004).
- <sup>34</sup>G. Franzò, A. Irrera, E. C. Moreira, M. Miritello, F. Iacona, D. Sanfilippo, G. Di Stefano, P. G. Fallica, and F. Priolo, *Appl. Phys. A: Mater. Sci. Process.* **74**, 1 (2002).
- <sup>35</sup>G. Franzò, V. Vinciguerra, and F. Priolo, *Appl. Phys. A: Mater. Sci. Process.* **69**, 3 (1999).
- <sup>36</sup>JCPDS Card No. 35-0297.
- <sup>37</sup>JCPDS Card No. 15-0886.
- <sup>38</sup>J. Lægsgaard, *Phys. Rev. B* **65**, 174114 (2002).